

Amendments To The Specification

1. Beginning on Page 30, Line 20:

Figures 6(~~A&B~~) (A-C) illustrate stopping liquid at a hydrophobic patch inside a microchannel. (A-C) shows a schematic of the procedure. (~~B~~) (C) shows micrographs of the actual mechanism.

2. Beginning on Page 51, Line 23:

Figures 6(A-C) presents a liquid drop ($\sim\mu\text{l}$) placed at the inlet hole using a pipette (Figure 6(i) A). The liquid is drawn inside the microchannel by capillary forces and is stopped at the hydrophobic patch (Figure 6(ii) B). (Figure 6C(e)) Photograph of a microchannel ($100 \mu\text{m} \times 20 \mu\text{m}$) device showing liquid being stopped at the hydrophobic patch ($200 \mu\text{m}$ wide). The ability of a hydrophobic patch to stop liquid inside a microchannel (Figures 6A-C) can be ascertained by studying the net pressure acting on the liquid inside the microchannel after the advancing liquid front has reached the hydrophobic patch (Figure 6(ii)B). A positive pressure difference is required for additional liquid to flow from the inlet hole over the hydrophobic patch. In order for the hydrophobic patch to stop the flow of liquid from the reservoir, the pressure difference, ignoring gravity effects, must be equal to or less than zero:

3. Beginning on Page 56, Line 5:

Figure 9 presents plots where the inlet pressure is balanced by the pressure at the hydrophobic patch. In order for liquid to be stopped at the patch (contact angle θ_p), the liquid volume should be higher than that on the plot for a given channel depth. Figure 9 also plots lines of $P_{l,i} - P_{l,a} = 0$ for different channel depths and a top contact angle (θ_t) of 90° . For a given patch contact angle (θ_p), there exists a threshold drop volume which lies on the ($P_{l,i} - P_{l,a} = 0$) lines for different channel depths. The liquid volume should be higher than the threshold amount for the hydrophobic patch to stop liquid. Mechanical pipetters, used routinely in laboratories can pipette drops as small as a microliter with an accuracy of half a microliter. For such drop volumes (few μl), a contact angle of 100° is high enough to stop

liquid in microchannels with depths below 60 μm , as observed in experiments (Figures 6A-C) and predicted by theory (Figure 9).

3. Beginning on Page 68, Line 29:

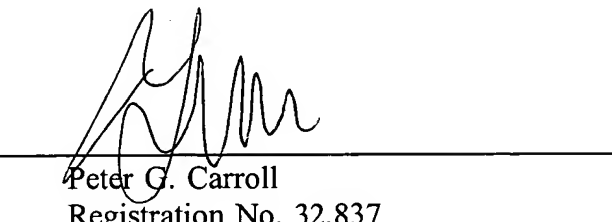
Based on flow visualization studies in a number of geometries, we selected cavities 1.5 cm in height with $h/d \sim 10$ for PCR experiments because of their characteristically slow flow velocities which permit adequate time to be spent within each temperature zone. The PCR mixture was subjected to convective flow generated with top and bottom surfaces of the cavity maintained at 61 °C and 97 °C, respectively. The bottom surface temperature was maintained with a heat source (*e.g.*, a hot plate) while the top surface temperature was maintained by circulating water from a water bath maintained at the correct temperature. Approximately 9 ng/ml of human DNA template was used and the target was a 295 bp (base pair) fragment of the single-copy beta-actin gene. Briefly, a 295-bp segment of the human β -Actin gene was amplified. Forward and reverse primer sequences were 5'-TCACCCACAATGTGCCCATCTACGA-3' (SEQ ID NO: 1) and 5'-CAGCGAACCGCTCATTGCCAATGG-3' (SEQ ID NO: 2). Reactions contained 10 mM Tris-HCL (pH 8.3); 50 mM KCL; 4 mM MgCl₂; 0.2 mM each dATP, dGTP, dCTP and dUTP; 9 ng/ μl human DNA and 0.1 U/ μl of AmpliTaq Polymerase (PE Applied Biosystems). Reactions were run for about 1.5 hours, aspirated from the reaction chambers, stained with SYBR-Green 1 (final concentration 200x) and run on a 1 % Agarose gel at 110 V for 1 hour. As shown in Figure 16C, the Rayleigh-Bénard cell was capable of producing an amplification product of the correct size and compares well with the PCR product generated in a thermocycler under similar temperature conditions. In addition to enzyme concentration, the reaction was sensitive to incubation time and the temperature at the top surface of the cell.

4. Beginning on Page 69, Line 21:

This successful demonstration of DNA amplification in a RB-PCR cell shows that Rayleigh-Bénard convection can serve as a useful platform to perform a variety of chemical and biochemical reactions which require temperature cycling. The system is exceedingly simple and may be easily assembled in any laboratory. The potential versatility of this system may be better realized through more thorough characterization, both theoretical and

experimental, of convective flow fields in high aspect ratio cavities and studies to optimize PCR in flowing systems. Addressing these issues presents a unique opportunity to attain an improved understanding of the fundamental physical processes governing PCR in static and flowing systems alike, while achieving DNA amplification in a greatly simplified experimental format. Specifically, Figure 16(B)C shows the result of DNA amplification in RB-PCR cell. The top and bottom surfaces of the cavity are maintained at $T_1 = 61^{\circ}\text{C}$ and $T_2 = 97^{\circ}\text{C}$, respectively. Human genomic DNA was used as template. (i) Amplification with 0.1 U/mL AmpliTaq Polymerase. Lane 1: 100 bp ladder, Lane 2: PCR product from RB-PCR cell, Lane 3: PCR product generated in a thermocycler using two-temperature cycling (denature: 95°C , anneal 61°C , 40 cycles). (ii) Negative control with no enzyme. Lane: 1 RB-PCR cell product, Lane 2: thermocycler product. (iii) Negative control with no enzyme. Lane 1: RB-PCR cell product, Lane 2: thermocycler product. (iv) Amplification with 0.15 u/mL AmpliTaq Polymerase. Lane 1: 50 bp ladder, Lane 2: PCR product from RB-PCR cell Lane 3: PCR product generated in a thermocycler using two-temperature cycling (denature: 95°C , anneal 61°C , 40 cycles). The intense high-migrating band observed in the RB-PCR positive reactions and template-containing negative control is likely to be an effect of high-temperature at the bottom of the cell (97°C) causing single-stranded scission of the >50 kb template DNA fragments (Lindahl, T., and B. Nyberg, *Biochemistry* 11:3610, 1972). A faint band is also observed at the same migration distance in positive reactions and template-containing negative controls generated in the thermocycler but does not appear in the photographs.

Dated: March 30, 2004



MEDLEN & CARROLL, LLP
101 Howard Street, Suite 350
San Francisco, California 94105
617.984.0616